THE ASTROPHYSICAL JOURNAL, 282:236–244, 1984 July 1

IR GEMINORUM: INDICATIONS OF A MASSIVE WHITE DWARF AND A HEATED SECONDARY IN THIS NEW SU URSAE MAJORIS CATACLYSMIC VARIABLE

PAULA SZKODY[1]
Department of Astronomy, University of Washington

ALLEN W. SHAFTER
Department of Astronomy, University of California, Los Angeles

AND

ANNE P. COWLEY
Department of Astronomy, University of Michigan
Received 1983 August 22; accepted 1984 January 12

ABSTRACT

We report the discovery of a new SU UMa type cataclysmic variable through confirmation of a 102 minute superhump period during a supermaximum. The superhump has a 30% color-independent amplitude with a decrease in the equivalent widths of the Balmer absorption lines.

Spectroscopic and photometric studies during quiescence show a 98–101 minute orbital period with evidence for heating of the secondary star. The flux distribution from 0.1 to 1.25 μm fits with a 20,000 K heated blackbody (or an $\dot{M} = 10^{-9}$ $M_\odot$ yr^{-1} Williams and Ferguson accretion disk model). The low semiamplitude of the radial velocity curve implies a high mass white dwarf and possibly a degenerate secondary, but may be complicated by an unresolved component in the emission lines.

Subject headings: stars: binaries — stars: dwarf novae — stars: individual

I. INTRODUCTION

The SU UMa stars are characterized by two types of outbursts. The normal outbursts are relatively short in duration (usually 1–2 days) and generally recur on time scales less than a month. The superoutbursts characteristically last about 5 times longer than the normal ones, are slightly brighter, and recur on longer time scales (about once a year). During the superoutbursts and only during the superoutbursts, periodic humps (superhumps) of about 30% amplitude are apparent in the orbital light curve on time scales a few percent longer than the orbital period. This hump cannot be a geometrical effect because it occurs in all systems regardless of the inclination. Of the various proposed models (summarized in Patterson 1979; Vogt 1980, 1982) the one with the least objections involves the presence of an eccentric disk at supermaximum. As this disk turns, the impact of the stream occurs at varying distances from the white dwarf, thus resulting in a modulation of the light curve from the varying kinetic energy of the impact stream. The sparse spectroscopic studies have shown broad Balmer absorption at supermax, as occurs at normal maximum. The strength of the Balmer absorption is correlated with the superhump in Z Cha (Vogt 1982) which is an eclipsing system, but there is no variation in the lower inclination system VW Hyi (Vogt 1976).

After 2 years of work on IR Gem at quiescence, we were fortunate to observe this system at superoutburst and discover superhumps which positively identify it as a SU UMa type. Table 1 summarizes the periods of the 14 known SU UMa stars—IR Gem is at the short period end of this group. Analysis of the AAVSO light curves of IR Gem from 1974 to 1977 (compiled by J. Mattei 1983, private communication) shows normal outbursts of 1–2 days at 20 day intervals and superoutbursts of >6 days duration at 135–172 day intervals.

TABLE 1

KNOWN SU URSAE MAJORIS VARIABLES

Star	P(sh) (minutes)	P(orb) (minutes)	References
V436 Cen	92	90	1, 2
OY Car	93	91	3
EK TrA	94	...	4
RZ Sge	101	...	5
TY Psc	101	...	6
IR Gem	102	101	...
AY Lyr	109	...	7
VW Hyi	111	107	8, 9, 10
Z Cha	111	107	11
WX Hyi	112	108	12
SU UMa	...	106–114	13
CU Vel	115	...	14
YZ Cnc	133	124	7, 15
TU Men	182	169	16, 17

REFERENCES.—(1) Semeniuk 1980. (2) Gilliland 1982*a*. (3) Vogt *et al.* 1981. (4) Vogt and Semeniuk 1980. (5) Bond, Kemper, and Mattei 1982. (6) Mattei 1982. (7) Patterson 1979. (8) Vogt 1974. (9) Vogt 1983. (10) Heafner *et al.* 1979. (11) Vogt 1982. (12) Schoembs and Vogt 1981. (13) Wade and Oke 1982. (14) Vogt 1980. (15) Shafter 1983*c*. (16) Stolz and Schoembs 1981*a*. (17) Stolz and Schoembs 1981*b*.

[1] Guest Investigator, Kitt Peak National Observatory, operated by AURA, Inc., under contract with the National Science Foundation, and with the *International Ultraviolet Explorer Satellite*.

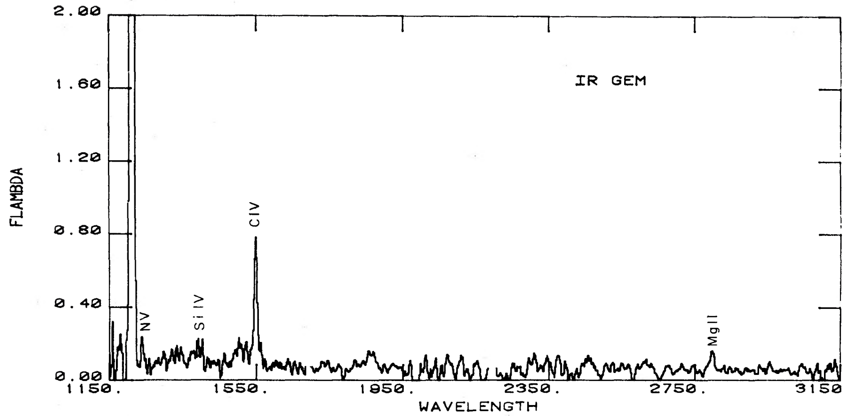

FIG. 1.—The combined and five point smoothed SWP and LWR spectra obtained with *IUE*

In this paper, we discuss the supermaximum properties of IR Gem as well as spectroscopic and photometric determinations of its quiescent characteristics.

II. OBSERVATIONS

a) *Ultraviolet* (*1150–3000 Å*)

The *IUE* satellite was used to observe IR Gem near quiescence on 1980 December 10 using the large aperture and low-dispersion mode. The SWP exposure was 120 minutes and the LWR lasted 60 minutes. The FES magnitude was estimated at 15.6, although it is very inaccurate at this low light level. The AAVSO circular indicates an outburst occurred on December 5, and since they generally last 1–2 days, IR Gem was probably at quiescence on December 10.

The spectra were too weak to make an accurate determination of the reddening. Figure 1 shows a smoothed spectrum with strong emission from C IV 1550 and weaker emission from N V 1240, Si IV 1396, 1403 and Mg II 2800. This is a typical spectrum for dwarf novae at quiescence (Szkody 1981; Krautter *et al.* 1981).

b) *Optical Photometry*

Light curves of several hours duration were obtained of IR Gem at quiescence on three consecutive nights in 1981 October at Kitt Peak, using the three channel photometer on the 1.3 m telescope. This photometer, which simultaneously measured *U*, *B*, and *V*, was unfortunately retired so that later observations of the supermaximum (1982 October) had to be made with the KPNO (MK2) photometer which cycled between filters with an automated wheel. Integration times of 10 s were used at quiescence and 2 s at supermaximum with associated statistical uncertainties of ≤ 0.02 mag. On 1982 October 13, an error was found in the computer software which disabled the dome tracking at short integration times so that all of the magnitudes could not be trusted but the times of superhumps could still be salvaged. Figures 2 and 3 show representative light curves at quiescence and supermaximum.

c) *Optical Spectroscopy*

Spectrophotometry at quiescence shows strong Balmer lines in emission. Spectra were obtained with the IIDS system on the KPNO 2.1 m telescope in a remote observing mode and also at Mount Lemmon with the ITS system on the 1.5 m telescope. The Kitt Peak data were obtained in photometric, good seeing conditions with a large apperture (8″4) so that the fluxes should be accurate to about 10%. The wavelength region was 3500–5300 Å with 9 Å resolution. The ITS was used at low resolution (11 Å) in 1982 January to obtain coverage from 3800 to 7000 Å (Fig. 4) while a higher resolution mode (4 Å) centered on Hα was used for a radial velocity determination of the orbital period on two nights in 1982 November. The time resolution of each spectrum was 8 minutes which was later binned for better signal-to-noise ratio.

During supermaximum, simultaneous with the broad-band photometry, seven spectra were obtained with the Mark II reticon on the McGraw-Hill Observatory 1.3 m telescope. At this time, the Balmer lines were in absorption (Fig. 5)

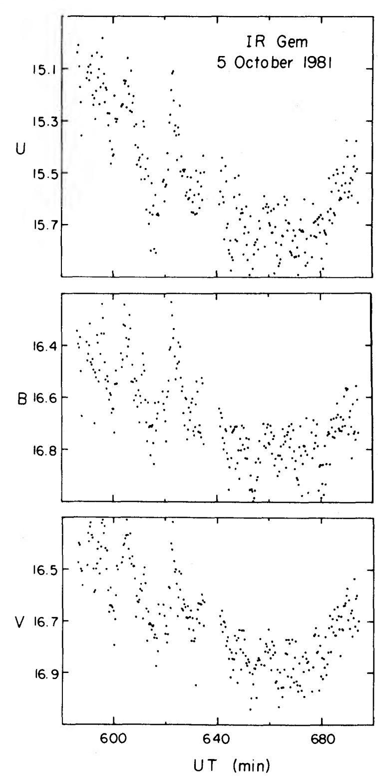

FIG. 2.—An example of the simultaneous *UBV* photometry of IR Gem at quiescence. Each point represents a 10 s integration.

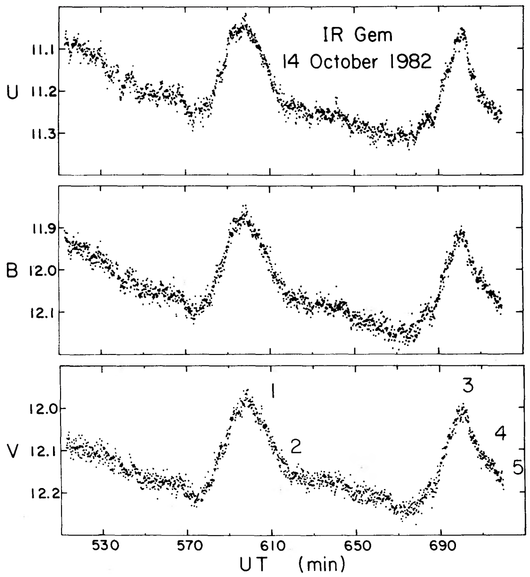

FIG. 3.—The light curve of IR Gem at supermaximum. Each point is a 2 s integration, and filters were cycled through U, B, and V.

as is typical for dwarf novae at outburst. Table 2 lists the times and phases of the spectra, while the numbers in Figure 3 refer to the appropriate simultaneous spectra obtained during the photometry.

d) *Infrared Photometry*

Broad band photometry from 1.25 to 2.2 μm was accomplished at a normal maximum and decline in 1981 October, and limits to J at quiescence were obtained in 1981 and 1983 with the Kitt Peak 1.3 m telescope and InSb system Otto. One sigma error bars were typically 0.1 mag. One orbit was covered at the J filter during maximum but no significant variability was evident.

Table 3 summarizes all of the available observations.

III. RESULTS

a) *Supermaximum*

The two superhumps observed on October 14 (Fig. 3) and the well-defined one observed October 13 determine a superhump period of 102 minutes. The amplitude is 30% in U, B, and V (the $U-B$ and $B-V$ curves are flat throughout the October 14 data period). This lack of color variation is common (Vogt and Semeniuk 1980) and indicates that the hump is not due to a specific temperature component, such as a hot spot. The asymmetric shape of the hump is very similar to those observed in EK TrA (Vogt and Semeniuk 1980). The determination of the orbital period

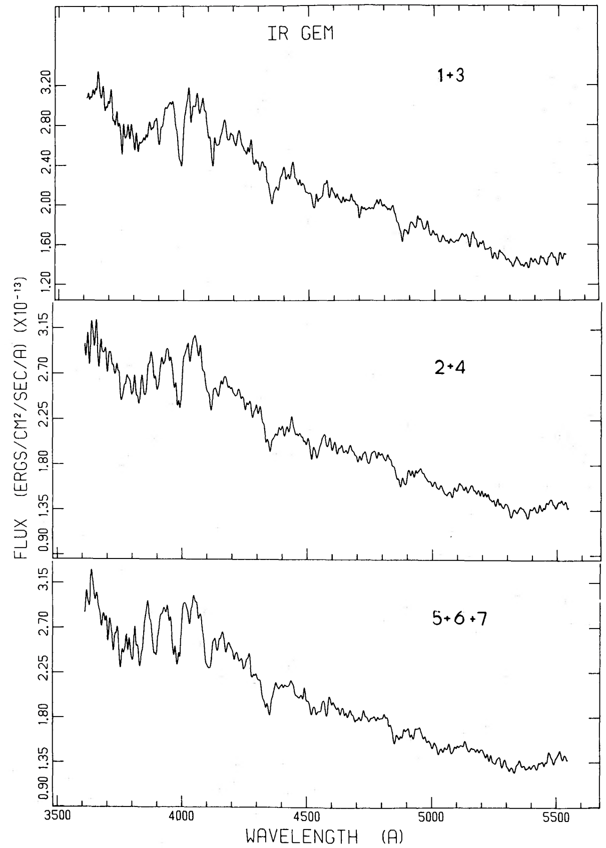

FIG. 5.—The supermaximum spectra obtained at the McGraw-Hill Observatory. The original seven spectra have been added by phase to increase the signal-to-noise ratio. The numbers refer to the identifications in Table 2.

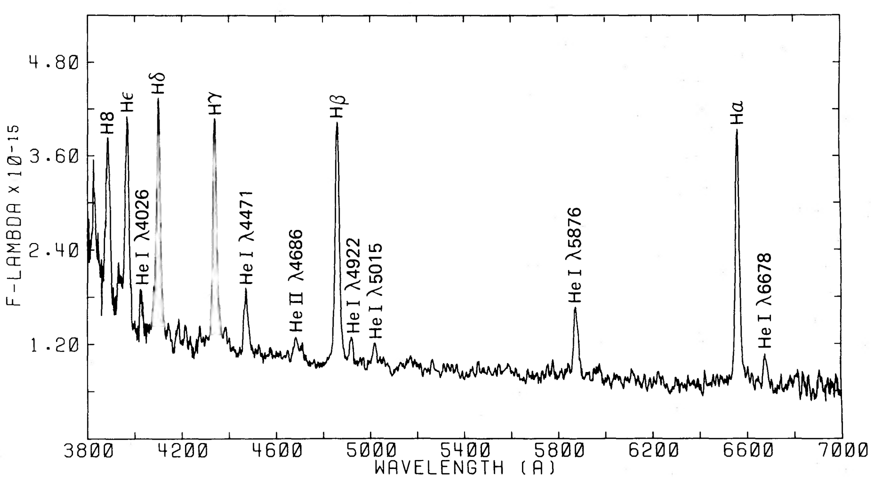

FIG. 4.—A typical 24 minute low resolution (11 Å) spectrum of IR Gem at quiescence obtained at Mount Lemmon

TABLE 2

SUPERHUMP SPECTRA

Scan	UT Start Time (minutes)	Exposure (minutes)	Superhump Phase[a]
1	611	7.6	0.11–0.19
2	621	6.5	0.20–0.26
3	703	5.8	0.00–0.06
4	721	7.1	0.17–0.24
5	729	5.7	0.26–0.32
6	736	8.1	0.33–0.41
7	745	7.6	0.42–0.50

[a] Phase 0 = superhump peak = JD $2,445,256.9160 \pm 7 + 0.07076E \pm 5$.

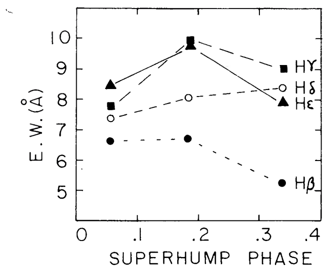

FIG. 6.—The variations of the equivalent widths of the Balmer absorption lines in the supermaximum spectra. Error bars are estimated to be on the order of 1 Å.

(§ III*b*) brings the number of systems with known superhump and spectroscopic periods to eight. In all of these, the supermaximum period is a few percent longer than the orbital period (Table 1).

There is no dramatic change evident in the spectra taken during the superhump versus the flat portion of the light curve. Figure 5 shows the addition of spectra 1 and 3 (taken during the hump), spectra 2 and 4 (during the hump decline), and spectra 5, 6, and 7 (during the flat portion). Figure 6 shows the measured equivalent widths of the hydrogen absorption lines during each of these three summed spectra. The equivalent widths are generally weakest at the peak of the hump, strongest at decline, and drop off again during the flat portion of the light curve. This can be understood in a straightforward way. At the peak of the hump, the continuum is strongest, which makes the equivalent widths small. As the system fades, the lines have about the same shape, but the continuum is lower, so the equivalent widths are larger. The decrease at the flat portion may be due to the changing strength of the hydrogen emission (see § III*b* [ii]) which weakens the absorption.

The width of the hydrogen absorption lines at supermaximum (full width zero intensity of about 50 Å) is similar to the full width of the emission lines at quiescence and implies a similar origin in the disk.

b) *Quiescence*

i) *Light Curves*

The three nights of photometry at quiescence all reveal the presence of a modulation that is approximately sinusoidal with flickering superposed (Fig. 2), although the exact shape varies from night to night. The only period near 102 minutes (the supermaximum period) that is consistent with this modulation is 101 ± 0.5 minutes. Table 4 lists the times of hump maxima that are consistent with this period for the photometry and spectrophotometry. The absence of an eclipse but the presence of the large mudulation generally implies an inclination in the range 45–60° (although invoking special disk geometries may yield a modulation for smaller inclinations).

Due to the flickering extent, it is difficult to tell if the modulation is strictly sinusoidal (associated with heating of the secondary) or due to the hot spot on the disk which is alternatively in the line of sight and hidden by the disk (as occurs in VW Hyi). The color of the bright portion of the modulation is blue (U amplitude above the lowest point = 0.6–0.9 mag; B amplitude = 0.4–0.7 mag; and V amplitude = 0.4–0.6 mag—Fig. 2). There is no extended flat portion in the light curves, and the faintest times occupy about 40% of the orbit. Further details of this modulation are

TABLE 3

SUMMARY OF OBSERVATIONS

UT Date (m-d-y)	Observatory	Instruments	State	Comments
12–10–80	*IUE*	SWP, LWR	min	SWP = 120 min, LWR = 60 min, FES > 15.6
10–03–81	KPNO 1.3 m	3 ch. phot.	min	2 hr (338 pts), $U = 15.33$, $B = 16.58$, $V = 16.60$
10–04–81	KPNO 1.3 m	3 ch. phot.	min	2 hr (306 pts), $U = 15.33$, $B = 16.59$, $V = 16.60$
10–05–81	KPNO 1.3 m	3 ch. phot.	min	2 hr (288 pts), $U = 15.54$, $B = 16.67$, $V = 16.70$
10–06–81	KPNO 1.3 m	Otto	min	$J > 16.5$
10–08–81	KPNO 1.3 m	Otto	max	90 min at J, $J = 12.8$, $H = 12.8$, $K = 12.9$
10–09–81	KPNO 1.3 m	Otto	decline	$J = 14.2$, $H = 13.9$, $K = 13.9$
01–28–82	Mount Lemmon	ITS	min	1 low res. spectrum over 24 min
10–06–82	KPNO 2.1 m	IIDS	min	2 low res. spectra over 36 min
10–08–82	KPNO 2.1 m	IIDS	min	4 low res. spectra over 80 min
10–13–82	KPNO 1.3 m	MK2 phot.	smax	2 hr (925 pts), $U = 11.27$, $B = 12.06$, $V = 12.15$
10–14–82	KPNO 1.3 m	MK2 phot.	smax	3 hr (1285 pts), $U = 11.20$, $B = 12.04$, $V = 12.14$
10–14–82	McGraw-Hill	Ret. scan.	smax	7 low res. spectra over 2 hr
11–13–82	Mount Lemmon	ITS	min	16 high res. spectra over $4\frac{1}{2}$ hr
11–14–82	Mount Lemmon	ITS	min	15 high res. spectra over $2\frac{1}{2}$ hr
02–21–83	KPNO 1.3 m	Otto	min	$J > 14.9$
02–22–83	KPNO 1.3 m	Otto	min	$J > 13.9$

TABLE 4

QUIESCENT CONTINUUM MAXIMA[a]

Source	Time (JD 2,440,000+)
Photometry	4880.958
Photometry	4881.937
Photometry	4882.919
IIDS	5249.037
IIDS	5250.931

[a] This is defined to be phase 0.5.

revealed from the study of the emission line changes (§ III*b* [ii]) and argue for a heating origin.

The flickering is largest during the bright portion (0.8 mag in *U* vs. 0.4 mag at the low portion of the light curve). This is similar to what is typically seen in a hot spot variation (Warner and Nather 1971), but it could also be consistent with a heating effect if the heated secondary is a flickering source.

ii) *Radial Velocities and Line Fluxes*

The 31 individual 8 minute spectra were used to derive a radial velocity curve from the Hα emission lines using the method of Shafter (1983*a*) which is based on double Gaussian fitting of the line wings. Due to the faintness of the source for the 1.5 m telescope, the data are marginal for the determination of a good spectroscopic solution. The individual spectra were used to derive the best fit period and then the spectra were coadded in 10 phase bins to improve the signal-to-noise in order to determine the amplitude. The derived orbital elements are given in Table 5, and the radial velocity curve is shown in Figure 7. The best fit spectroscopic period of 98.5 ± 0.4 minutes is marginally consistent with the photometric period from the quiescent modulation. Due to the longer time base of the photometry and the difficulty in doing the spectroscopic measurement, we will assume the binary period is 101 minutes throughout the rest of the discussion.

Assuming the radial velocity curve represents the motion of the primary, the small value of $K_1 = 30$ km s^{-1} implies either (*a*) a low orbital inclination (not likely due to the presence of the modulation in the light curve) or (*b*) a massive WD or a very low mass secondary. Alternatively, the emission may not be directly associated with either star. If we assume that the Hα line does originate from the inner disk close to the dwarf, we can try to place some limits on the masses. Because of the limitations of short orbital period, telescope size, and faintness of the system at quiescence, the available spectra were too noisy to apply the modified Warner method to the mass determination using a good

TABLE 5

SPECTROSCOPIC ORBITAL ELEMENTS

Element	Value
P	0.06837 + 0.00031 days
T	2,445,286.9126 ± 0.0035 days
K_1	30 ± 4 km s^{-1}
γ	0
e	0 (assumed)
ω	0 (assumed)

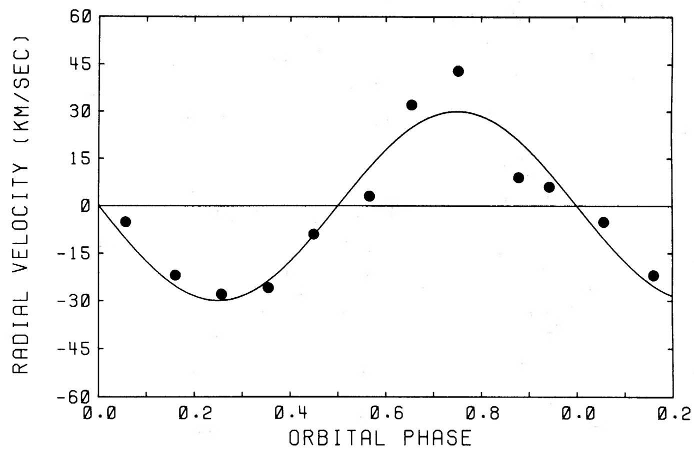

FIG. 7.—The radial velocity curve obtained from the high-resolution Hα emission-line data. Each point is the result of co-adding the 31 individual 8 minute spectra into 10 phase bins.

estimate of K_1 and $v_d \sin i$ as in Shafter (1983*a*). Instead, we may only make some crude estimates.

Under the assumption that the secondary fills its Roche lobe and is a main sequence star, the standard relations (Warner 1976) give an estimate of the secondary mass in solar masses:

$$M_2 = 3.18 \times 10^{-5} P ,$$

where P is the period in seconds and $q < 0.5$. This results in $M_2 \approx 0.19\ M_\odot$. For any inclination $> 30°$, the mass function ($1.91 \times 10^{-4}\ M_\odot$) yields $M_2 < 0.2\ M_\odot$ for a white dwarf mass less than 1.4 $M_\odot$. (At $i = 30°$ and $M_1 = 1.2\ M_\odot$, $M_2 = 0.14\ M_\odot$). A lower limit to M_1 can be estimated by requiring that the maximum velocity of the line wings is not greater than the Keplerian velocity at the white dwarf:

$$(GM_1/R_1)^{1/2} \sin i > 1550 \text{ km s}^{-1} ,$$

where this velocity comes from the half-width at zero intensity of Hα (25 Å). Using the mass-radius models for white dwarfs from Hamada and Salpeter (1961) gives $M_1 > 0.25\ M_\odot$ for $i = 60°$ and $M_1 > 1.3\ M_\odot$ for inclinations that are about 10°. We note that these lower limits are not very stringent because of the possibility that the emission lines are broadened by other processes besides Doppler motions, e.g., pressure broadening. Using Warner's method:

$$K_1/v_d \sin i = qf^2(q) ,$$

with $v_d \sin i$ being somewhere near the HWHI (7–10 Å) gives q in the range of 0.1–0.2 which implies $M_1 > 1\ M_\odot$, for a main-sequence secondary. For the highest possible mass value ($M_1 = 1.4\ M_\odot$), $q = 0.14$. However, with this q value, the estimate of the inclination (Warner 1976):

$$\sin i = 3.35 \times 10^{-8} K_1 (1 + 1/q)^{2/3}$$

yields about 25°, which is not consistent with the modulation seen in the light curve (even if this is a heating effect, i must be on the order of 45°) or with the large line widths of 3100 km s^{-1} full width zero intensity, unless pressure broadening is important. In summary, the small observed value of K_1 is not consistent with the strong photometric modulation seen in the light curve unless the mass ratio is extreme (i.e., $q \lesssim 0.1$). This small mass ratio

TABLE 6

ORBITAL ELEMENTS OF ULTRASHORT PERIOD DWARF NOVAE

Object	P(min)	K_1 (km s^{-1})	Hα HWZI (km s^{-1})	$M_2(M_\odot)$	$M_1(M_\odot)$	i (degrees)	Reference
SW UMa	82	47	2000	<0.15	>0.4	30–65	1
T Leo	85	135	1900	0.19	0.4	28–65	2
V436 Cen	90	59	...	0.14	0.9	40–65	3
OY Car	91	85	2100	0.14	1.0	80	4
HX Hya	98	58	3500	0.17	1.4	75	5
IR Gem	101	30	1550	0.19	1.4	45–65	...
HT Cas	106	115	...	0.19	0.53	76	6
VW Hyi	107	78	1120	0.11	0.6	60	7
Z Cha	107	87	2300	0.17	0.9	79	8
WX Hyi	108	67	1045	0.16	0.9	40	7

REFERENCES.—(1) Shafter 1983*b*. (2) Shafter and Szkody 1984. (3) Gilliland 1982*a*. (4) Schoembs and Hartmann 1983 (5) Gilliland 1982*b*. (6) Young, Schneider, and Shectman 1981. (7) Schoembs and Vogt 1981. (8) Vogt 1982.

implies a massive white dwarf for reasonable estimates of the secondary mass. The relevant parameters for similar period systems are listed in Table 6.

One alternative to the proposition that q is very small could be provided by the presence of a narrow-line component which is unresolved in our available data but which is affecting the measured semiamplitude of the velocity curve. At least two short period systems, i.e., T Leo (Shafter and Szkody 1984) and HT Cas (Young, Schneider, and Shectman 1981), are known to have a peak component that is 230° out of phase with the base. One suggestion for the origin of this offset component is an interaction with a wind emanating from the secondary. Another possibility is a component from the heated face of the secondary. The effect of another component like this to the lines could greatly affect the K_1 value obtained (although the data points are surprisingly well constrained with the small amplitude, yielding a formal error of only 4 km s^{-1}!). If K_1 is actually near 50 km s^{-1}, then q can go up to about 0.3. Although our data do not allow us to precisely determine M_1, we can be fairly confident that it is a high mass white dwarf.

If the low-velocity amplitude is real (and from the WD), we are left to consider the intriguing possibility that the secondary in IR Gem may be a low-mass degenerate star so that the mass ratio of the system is actually near 0.05. The evolutionary tracks of Paczyński and Sienkiewicz (1981, 1983) show that low-mass main-sequence stars may evolve to a minimum period through the effects of gravitational radiation and then start a period increase as a degenerate star. Thus, for a given period for short period systems, there is actually a dual solution for the secondary mass. For a period of 101 minutes, the secondary in IR Gem could be either a 0.14 $M_\odot$ main-sequence or a 0.03 $M_\odot$ degenerate star. With a q value of 0.05, the inclination comes up to 50°, which is more consistent with the light curve.

Further information on the complexity of the situation in IR Gem comes from the study of the line fluxes throughout the orbit. As apparent in Figure 8, the line fluxes undergo a change throughout the orbit. Table 7 summarizes the equivalent widths and hydrogen and helium line fluxes during the four phase bins obtained with the IIDS data on 1982 October 8 (photometric conditions with a large aperture). Also included are the continuum fluxes at 3600 and 5000 Å. It is apparent that the source of the continuum brightening is also the source of the He II emission and a dominant contributor to the He I and Balmer line emission. Within these four phase bins, the 3600 Å continuum changes by a factor of 2.25, the 5000 Å flux by a factor of 2 (consistent with the *UBV* curves), the Hβ flux by 3.4, and He I 4471 by a factor of 4. Although the ITS data on Hα were not photometric, the equivalent widths display the same effect as the higher Balmer lines, with the equivalent width of Hα changing by a factor of 1.2 over the orbit (Fig. 9). This type of behavior is more reminiscent of the accretion area in VV Pup (Schneider and Young 1980) than systems with a normal hot spot (Williams and Ferguson 1982). This latter

TABLE 7

HYDROGEN AND HELIUM LINE EQUIVALENT WIDTHS (Å) AND FLUXES ($\times 10^{-15}$ ergs cm^{-2} s^{-1}) FOR 1982 OCTOBER 8

	SCAN 1: ph. 0.50–0.60		SCAN 2: ph. 0.63–0.73		SCAN 3: ph. 0.77–0.01		SCAN 4: ph. 0.04–0.28	
WAVELENGTH	E.W.	Flux	E.W.	Flux	E.W.	Flux	E.W.	Flux
3600 Å	...	2.25	...	1.75	...	1.50	...	1.0
5000 Å	...	0.6	...	0.6	...	0.5	...	0.3
Hβ	116	84	115	54	73	38	71	25
Hγ	77	65	56	37	62	35	51	20
Hδ	53	53	46	35	47	31	25	13
He 4471	24	20	23	13	5	3	12	5
He II 4686	29	21	21	10	...	...	...	...

NOTE.—Phases computed for continuum maximum = phase 0.5 = JD 2,445,250.931 + 0.0701.
±4

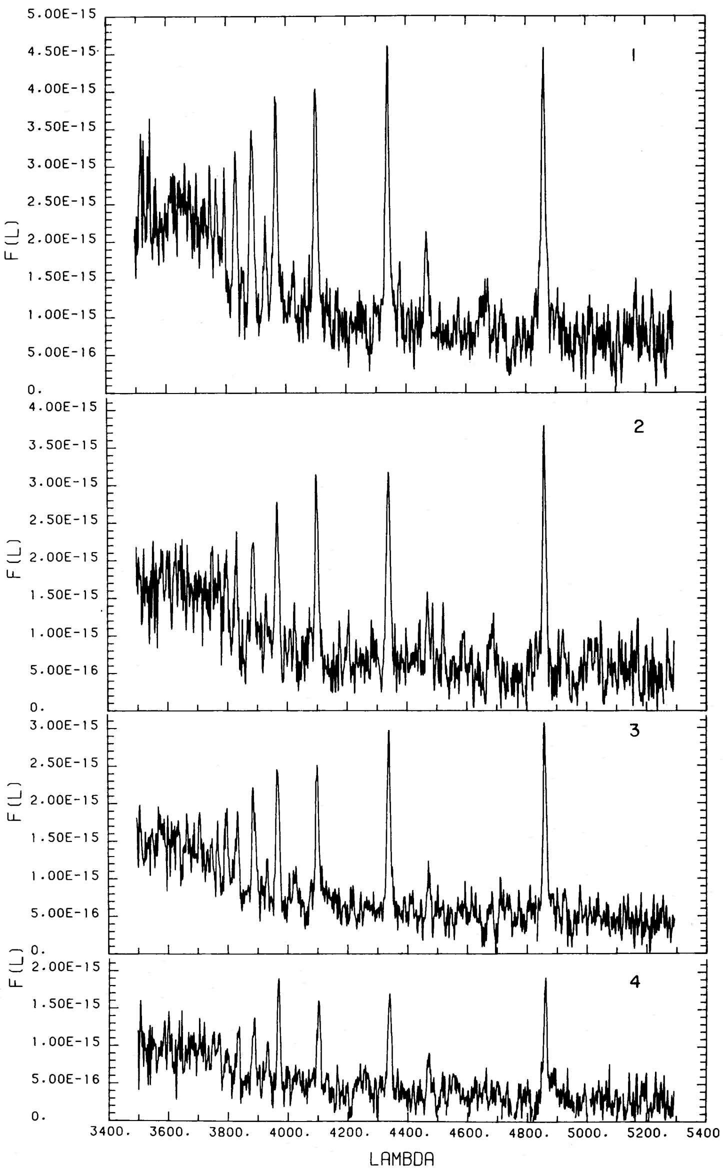

FIG. 8.—The IIDS spectra showing the orbital variation in the lines and continuum. The numbers refer to the scans listed in Table 7.

study of eclipsing systems showed that the hydrogen and He I lines were not eclipsed and were thus associated with the outer disk area, while He II was eclipsed and hence was associated with the inner disk or hot spot. However, in VV Pup and systems of its type, the He II 4686 is generally comparable to Hβ in strength, while in most of the dwarf novae, it is generally absent except near outburst. SU UMa

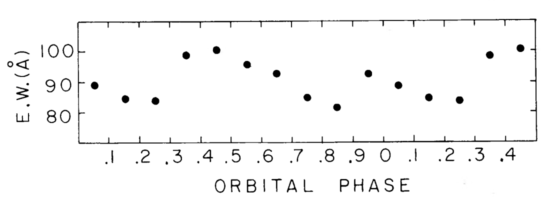

FIG. 9.—The orbital variation of the equivalent width of the Hα emission line. This is the same data used to construct the radial velocity curve. Errors are estimated to be 5 Å.

has He II 4686 at quiescence (Szkody 1981), but there is no known orbital variation (implying a low inclination) in order to study its origin. From the study of the eclipsing novalike system PG1012 (Penning *et al.* 1984), it is apparent that a hot spot can contribute a substantial amount to the He II flux.

We can use the phasing from the Hα data to locate the emission line source. If the Hα equivalent width variation (Fig. 9) is indeed mimicking the same variation evident in the IIDS data and the photometry for the higher order Balmer series and the continuum, then the spectroscopic phasing from the 10 phase bin ITS data implies that the major line source is seen at phase 0.5, where phase 0 is superior conjunction of the white dwarf. (There is also an increase near phase 0 which is a further argument for a two-component line source). This means that the maximum source contribution occurs when we are viewing the side of the secondary that faces the white dwarf. The implication of this result is that the major source of emission is gas near the inner Lagrangian point or that the secondary is heated by its close presence to the white dwarf and the modulation seen in the continuum and lines is due to viewing various sides of the secondary. Other short-period system like HT Cas, and T Leo do not show this heating effect, although T Leo and HT Cas have a sharp component of uncertain origin (Shafter and Szkody 1984). We would expect IR Gem to have a larger heating effect than the other system of similar period because its white dwarf appears to be more massive (by more than a factor of 2) so that its size is smaller and, therefore, the inner disk/accretion area is hotter. This reasoning is substantiated by the larger UV flux of IR Gem (§ III*c*) than T Leo (Shafter and Szkody 1984) and with the observed X-ray flux (Córdova, Jensen, and Nugent 1980).

Other cataclysmic variables showing a modulation of the continuum and lines from possible heating of the secondary are the DQ Her type systems H2252 and H2215 (Patterson and Price 1981; Patterson and Steiner 1983). In H2215, with a 4 hr orbital period, it is estimated that about 20% of the X-ray flux ($F_x \approx 3 \times 10^{-11}$ ergs cm^{-2} s^{-1}) is reprocessed. In IR Gem, the observed modulation shows that about 50% must be reprocessed. The observed X-ray flux from *HEAO 1* (3×10^{-11} ergs cm^{-2} s^{-1}—Córdova, Jensen, and Nugent 1980) is higher than that observed for other SU UMa systems like YZ Cnc and VW Hyi (Córdova, Mason, and Nelson 1981). Unfortunately, the same energetics problem as pointed out for H2215 by Patterson and Steiner (1981) exists for IR Gem. For a 0.2 $M_\odot$ secondary and a 1.2 $M_\odot$ white dwarf, a $\sim 4 \times 10^{10}$ cm. The fraction of solid angle occupied by the secondary in this situation is only about 2%, so that the actual high-energy X-ray flux should be about 50 times the observed optical reprocessed light. The total observed optical flux from 0.1 to 1.25 μm is 2×10^{-11} ergs cm^{-2} s^{-1} (§ III*c*) so that if 1×10^{-11} ergs cm^{-2} s^{-1} is reprocessed, then the expected X-ray flux is about 5×10^{-10} ergs cm^{-2} s^{-1}, which is about 10 times the observed portion. This is the same missing order of magnitude that is apparent in H2215 and H2252. Either all of these systems have a significant amount of flux in the unobserved portion of the soft X-ray/extreme UV or the heating is not occurring as we expect.

c) *The Flux Distribution*

Figure 10 shows all of the available data from the UV through the IR during the supermaximum, decline, and quiescence. These data are orbit averages. If the IR fluxes obtained at the maximum on 1981 October 8 are similar to those at a supermaximum, the flux distribution is quite steep ($F_\lambda \alpha \lambda^{-3}$ in the optical to $F_\lambda \alpha \lambda^{-4}$ in the IR). In AY Lyr near supermaximum, the UV flux was similar to the outburst flux distribution ($F_\lambda \alpha \lambda^{-2.3}$) but raised by a factor of 2. *IUE* data on IR Gem at supermaximum are needed to see if the UV flux distribution does the same. If so, and if this distribution really represents a steady state disk condition, it is possible that the steeper optical slope represents the turnover of the disk (where it becomes optically thin) at fairly hot temperatures compared to the usual temperature of 5000–7000 K. From Table 2, it is apparent that there is no red precursor of the outburst as occurs in VW Hyi (Hassall *et al.* 1983) at least to within 1 day. (The AAVSO records indicate that the maximum of IR Gem occurred on 1981 October 7, and the data obtained on October 6 showed no excess over the normal quiescent values).

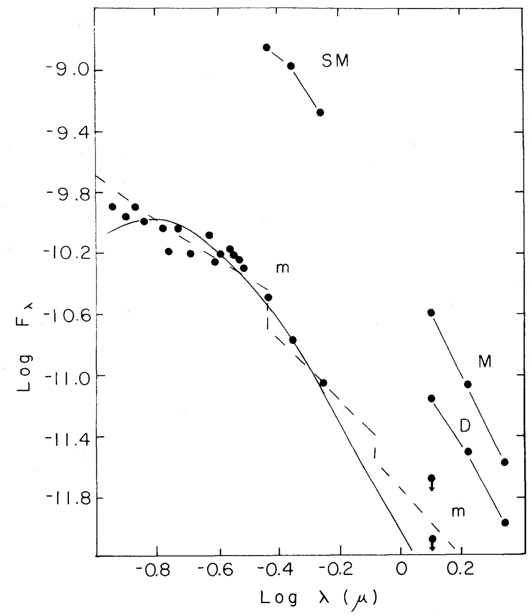

FIG. 10.—The flux distribution from UV through IR. SM refers to the optical supermaximum data, M and D to the IR data at a normal maximum and decline, and m to the minimum (quiescence) data. The solid line is the best fit blackbody ($T = 19{,}000$ K) and the dashed line is the best fit Williams and Ferguson (1982) disk model ($\dot{M} = 10^{-9}\ M_\odot$ yr^{-1}).

At quiescence, the distribution is much flatter ($F_\lambda \alpha \lambda^{-1}$) in the UV (and steeper in the optical with α index ≥ 2), implying a much lower accretion rate than at outburst. The best fit Williams and Ferguson (1982) model is near $\dot{M} = 10^{-9}\ M_\odot$ yr^{-1} (as shown in Fig. 10), but it is generally doubtful that the steady state disk models are applicable near quiescence (Cannizzo, Ghosh, and Wheeler 1982; Faulkner, Lin, and Papaloizou 1983).

Because of the possibility of a significant heating effect in the system, we also tried to fit the quiescent data with blackbodies. The best fit was obtained with $T = 19{,}000 \pm 1000$ K, which fits the data as well as the Williams and Ferguson disk model. It seems likely that this could be the temperature of the heated component, although time-resolved *IUE* and optical data will be needed to sort out this heated component from the other light contributions of the system (disk and white dwarf).

The other four SU UMa systems with published UV fluxes at quiescence, i.e., SU UMa, YZ Cnc, AY Lyr, and VW Hyi (Szkody 1981, 1982; Mateo and Szkody 1983), all show a two-component spectrum with a hot white dwarf or a steep power-law (alpha index ≥ 2) present in the short wavelength UV and a flatter component (possibly a low accretion rate disk) dominating the long wavelength UV and the optical. Although it has been suggested that T Leo could be an SU UMa type (Shafter and Szkody 1984), it does not reveal the presence of a hot component. However, its white dwarf is the least massive (Table 6), so that the inner disk should be the coolest.

IV. CONCLUSIONS

Our study of the outburst and quiescent properties of IR Gem have led to the following results:

1. IR Gem is a confirmed SU UMa type variable with a *superhump period* of 102 minutes. The superhump has a 30%

modulation independent of color. A small decrease in equivalent widths of the Balmer absorption lines during the superhump is consistent with the presence of a strong continuum at this time.

2. The *orbital period* of IR Gem is 101 minutes, although there is a slight difference between the spectroscopic and photometric determinations. Like six other SU UMa systems, the orbital period is a few percent shorter than the superhump period.

3. The low radial velocity amplitude of 30 km s^{-1} implies a massive white dwarf for the primary. It is possible the secondary is a low-mass degenerate star which is in an evolutionary state which has passed its minimum period. However, this low amplitude may reflect the combined motion of material near the white dwarf plus a second component from the heated face of the secondary or from between the stars. In this case, the white dwarf mass may be significantly lower than we have estimated.

4. The modulation of the *UBV* light curves and the phasing of the line flux variations imply that heating of the secondary star contributes a significant amount of light to this system.

5. The UV to IR flux distribution of IR Gem at quiescence can be equally well fitted with a 20,000 K blackbody (the heated secondary?) or a Williams and Ferguson (1982) model disk with a relatively high mass accretion rate of 10^{-9} $\dot{M}_{\odot}$ yr^{-1}.

Further high-resolution spectroscopy is needed to determine if there is a narrow component to the emission lines that is 180° out of phase with the broad base, as would be consistent with the heating of the secondary. This type of study could also resolve the 98 versus 101 minute period discrepancy from the photometric and spectroscopic data and determine if the low radial velocity amplitude is a result of a mixture of components. Time resolved simultaneous UV and optical fluxes over the orbit are needed to resolve what portion of the total flux comes from the disk and from a heated secondary. Finally, observations in the soft X-ray/near-UV region are needed to resolve the missing high-energy radiation that must exist if the observed light is indeed reprocessed radiation.

We gratefully acknowledge Dr. J. Mattei and the members of the AAVSO for the long-term light curves of IR Gem which helped in our determinations of the optical state of the system. In addition, A. W. S. would like to thank R. Nolthenius for his assistance at Mount Lemmon and P. B. Etzel for the use of his Spectroscopic Binary Orbit Program. The Kitt Peak telescope operators and staff were very helpful during the various types of optical/IR data acquisition and reduction, and the *IUE* operators and resident astronomers are acknowledged for their help with the *IUE* data. We thank Dr. N. Vogt for several valuable comments. This research was partially supported by NSF grant AST 82-04488 and NASA grant NSG 5395 for P. S. and NSF grant AST-83-12271 for A. P. C.. A. W. S. would like to thank Dr. R. K. Ulrich for financial support through NSF grant AST 78-20236.

REFERENCES

Bond, H. E., Kemper, E., and Mattei, J. A. 1982, *Ap. J.* (*Letters*), **260**, L79.
Cannizzo, J. K., Ghosh, P., and Wheeler, J. C. 1982, *Ap. J.* (*Letters*), **260**, L83.
Córdova, F. A., Jensen, K. A., and Nugent, J. J. 1981, *M.N.R.A.S.*, **196**, 1.
Córdova, F. A., Mason, K., and Nelsen, J. 1981, *Ap. J.*, **245**, 609.
Faulkner, J., Lin, D. N. C., and Papaloizou, J. 1983, preprint.
Gilliland, R. 1982*a*, *Ap. J.*, **254**, 653.
———. 1982*b*, *Ap. J.*, **258**, 576.
Haefner, R., Schoembs, R., and Vogt, N. 1979, *Astr. Ap.*, **77**, 7.
Hamada, J., and Salpeter, E. 1961, *Ap. J.*, **143**, 683.
Hassall, B. J. M., Pringle, J. E., Schwarzenberg-Czerny, A., Wade, R. A., Whelan, J. A. J., and Hill, P. W. 1983, *M.N.R.A.S.*, **203**, 865.
Krautter, J., Klare, G., Wolf, B., Deurbeck, H. W., Rahe, J., Vogt, N., and Wargau, W. 1981, *Astr. Ap.*, **102**, 337.
Mateo, M., and Szkody, P. 1983, *A.J.*, submitted.
Mattei, J. A. 1982, *Bull. AAS*, **14**, 879.
Paczyński, B., and Sienkiewicz, R. 1981, *Ap. J.* (*Letters*), **248**, L27.
———. 1983, *Ap. J.*, **268**, 825.
Patterson, J. 1979, *A.J.*, **84**, 804.
Patterson, J., and Price, C. M. 1981, *Ap. J.* (*Letters*), **243**, L83.
Patterson, P., and Steiner, J. E. 1983, *Ap. J.* (*Letters*), **264**, L61.
Penning, W. R., Ferguson, D. P., McGraw, J. T., Liebert, J., and Green, R. F. 1984, *Ap. J.*, **276**, 233.
Schneider, D. P., and Young, P. J. 1980, *Ap. J.*, **240**, 871.
Schoembs, R., and Hartmann, K. P. 1983, *Astr. Ap.*, in press.
Schoembs, R., and Vogt, N. 1981, *Astr. Ap.*, **97**, 185.
Semeniuk, I. 1979, *Astr. Ap. Suppl.*, **39**, 29.
Shafter, A. W. 1983*a*, *Ap. J.*, **267**, 222.
———. 1983*b*, *Inf. Bull. Var. Stars*, No. 2354.
———. 1983*c*, Ph.D. thesis, UCLA.
Shafter, A. W., and Szkody, P. 1984, *Ap. J.*, **276**, 305.
Stolz, B., and Schoembs, R. 1981*a*, *Inf. Bull. Var. Stars*, No. 1955.
———. 1981*b*, *Inf. Bull. Var Stars*, No. 2029.
Szkody, P. 1981, *Ap. J.*, **247**, 577.
———. 1982, *Ap. J.*, **261**, 200.
Vogt, N. 1974, *Astr. Ap.*, **36**, 369.
———. 1976, in *IAU Symposium 73, Structure and Evolution of Close Binary Systems*, ed. P. Eggleton, S. Mitton, and J. Whelan (Dordrecht: Reidel), p. 147.
———. 1980, *Astr. Ap.*, **88**, 66.
———. 1982, *Ap. J.*, **252**, 653.
———. 1983, *Astr. Ap.*, **118**, 95.
Vogt, N., and Semeniuk, I. 1980, *Astr. Ap.*, **89**, 223.
Vogt, N., Schoembs, R., Krzeminski, W., and Pedersen, H. 1981, *Astr. Ap.*, **94**, L29.
Wade, R. A., and Oke, J. B. 1982, *Bull. AAS*, **14**, 880.
Warner, B. 1976, in *IAU Symposium 73, Structure and Evolution of Close Binary Systems*, ed. P. Eggleton, S. Mitton, and J. Whelan (Dordrecht: Reidel), p. 85.
Warner, B., and Nather, R. E. 1971, *M.N.R.A.S.*, **152**, 219.
Williams, R. E., and Ferguson, D. P. 1982, *Ap. J.*, **257**, 672.
Young, P. J., Schneider, D. P., and Shectman, S. A. U. 1981, *Ap. J.*, **245**, 1035.

ANNE P. COWLEY: Department of Physics, Arizona State University, Tempe, AZ 85281

ALLEN W. SHAFTER: Department of Astronomy, University of Texas, Austin, TX 78712

PAULA SZKODY: Department of Astronomy, University of Washington, Seattle, WA 98195